A small molecule CRTH2 antagonist inhibits FITC-induced allergic cutaneous inflammation

Stefen A. Boehme[1], Karin Franz-Bacon[1], Edward P. Chen[1], Roman Šášik[2,3], L. James Sprague[2], Tai Wei Ly[1], Gary Hardiman[2,4] and **Kevin B. Bacon[1]**

[1]Actimis Pharmaceuticals, Inc., 10835 Road to the Cure, Suite 200, San Diego, CA 92121, USA
[2]Biomedical Genomics Microarray Facility, School of Medicine, University of California, San Diego, La Jolla, CA, USA
[3]Moore's Cancer Center, University of California, La Jolla, CA, USA
[4]Department of Medicine, University of California, La Jolla, CA, USA

Abstract

A FITC-induced allergic contact hypersensitivity model was used to investigate the role that the prostaglandin D_2 receptor–chemoattractant receptor-homologous molecule expressed on T_h2 cells (CRTH2) plays in modulating cutaneous inflammation. Our results show that inhibition of CRTH2, achieved via administration of a potent, small molecule antagonist, Compound A (Cmpd A), effectively blocked edema formation and greatly reduced the inflammatory infiltrate and skin pathology observed in drug vehicle-treated animals. Gene expression analysis revealed that Cmpd A administration down-regulated the transcription of a wide range of pro-inflammatory mediators. This correlated with decreases in cytokine and chemokine protein levels, notably IL-4, IL-1β, tumor necrosis factor-α, transforming growth factor-β, GRO-α, MIP-2 and thymic stromal lymphopoietin (TSLP) in FITC-challenged ears. The administration of an anti-TSLP-neutralizing antibody was only partially effective in lowering the FITC-induced inflammatory infiltrate and cytokine production compared with the CRTH2 antagonist. Taken together, these data suggest that blockade of CRTH2 inhibits multiple pathways leading to cutaneous inflammation in this model. This suggests that CRTH2 antagonism may be a viable route for therapeutic intervention in allergic skin diseases, such as atopic dermatitis.

Introduction

Atopic dermatitis (AD) is a common inflammatory disease of the skin that typically begins in early childhood, and patients often go on to develop other atopic diseases such as asthma and allergic rhinitis (1, 2). Clinical hallmarks of AD include severe pruritis, chronic eczematous skin lesions and epidermal thickening and hypertrophy (1, 3). Histological examination reveals an inflammatory infiltrate consisting predominantly of memory CD4+ T lymphocytes, and chronic lesions also display increased numbers of mast cells, eosinophils and IgE bearing Langerhans cells (2, 3). A number of clinical observations point to underlying immune abnormalities, as patients display elevated serum IgE levels, peripheral blood eosinophilia, greater numbers of CLA+ CRTH2+ CD4+ T cells in the circulation compared with control patients (4) and an increased expression of T_h2 cytokines, including IL-4, IL-5, IL-13 and tumor necrosis factor-α (TNF-α) (5). Recently, the cytokine thymic stromal lymphopoietin (TSLP) has been implicated as an initiating

factor in AD (6). TSLP has been shown to have the ability to polarize naive CD4+ T cells toward a T_h2 allergic phenotype and this is thought to be mediated by its effect on cutaneous dendritic cells. TSLP is expressed by epithelial cells, including keratinocytes, and its expression is induced by a wide range of stimuli including IL-1β and certain toll-like receptor ligands (7). Transgenic mice engineered to over-express TSLP in keratinocytes develop an AD-like phenotype, including eczematous lesions containing inflammatory dermal infiltrates and elevated serum IgE levels (8). Retinoid X receptor gene-deficient mice also develop a chronic dermatitis similar to AD, as keratinocytes in these animals over-express TSLP (9). Interestingly, as TSLP-treated dendritic cells induce the expression of IL-4 by T lymphocytes, transgenic mice expressing epidermal IL-4 develop an inflammatory skin disease reproducing many of the key features of human AD also (10). These transgenic models highlight the importance of TSLP and

IL-4 in the development of an inflammatory dermatitis similar to AD.

A mouse model for contact hypersensitivity induced by FITC has many features in common with acute AD lesions. Initial topical sensitization of mice to FITC resulted in increased IgE levels, as well as the development of FITC-specific T_h2 cells (11, 12). Antigen challenge by applying FITC to the ear 6 days post-sensitization results in cutaneous inflammation characterized by edema and a large infiltrate of mononuclear cells, eosinophils and neutrophils. This response has been shown to be dependent upon CD4^{+} T cells and IL-4, as the addition of anti-IL-4-neutralizing antibody significantly blocks edema formation. The treatment of mice with 48/80, a mast cell-depleting agent, also had a significant effect on reducing inflammation, demonstrating a mast cell dependence, in addition to CD4^{+} T cells, in this model (11).

Mast cell activation induced by the aggregation of antigen-specific IgE by polyvalent antigen triggers a signaling cascade resulting in the immediate release of secretory granules and the generation of arachidonic acid metabolites, cytokines and chemokines. The major arachidonic acid product made by mast cells is prostaglandin D_2 (PGD_2), and this prostenoid has been implicated in the development of various allergic diseases, such as AD, asthma and allergic rhinitis (13, 14). Two receptors have been identified for PGD_2, DP1 and chemoattractant receptor-homologous molecule expressed on T_h2 cells (CRTH2) (15). CRTH2 has amino acid sequence homology to chemokine receptors and like other chemoattractant receptors is a $G_{\alpha i}$-linked G protein-coupled receptor (14). CRTH2 binds PGD_2 with nanomolar affinity and has been shown to be expressed by T_h2 T lymphocytes, eosinophils and basophils in humans and also a subset of T_h1 T cells in the mouse (16–18). We investigate here the role of CRTH2 in a murine allergic contact inflammation model of human AD.

Materials and methods

Materials

All reagents were purchased from Sigma (St Louis, MO, USA) unless otherwise stated. The animal care and use committee (The Institutional *Animal Care and Use Committee*) approved all animal experimentation prior to implementation. BALB/c mice (females 4–6 weeks of age) were used in all the studies and were purchased from Harlan Sprague Dawley, Inc. (Indianapolis, IN, USA). Ramatroban and BW868c were purchased from Cayman Chemical (Ann Arbor, MI, USA). Compound A (Cmpd A) is a proprietary, highly potent and selective CRTH2 small molecular weight antagonist that was developed as part of the Actimis Pharmaceuticals, Inc. portfolio of potent and selective compounds (WO/2004/096777). The IC_{50} values of Cmpd A inhibiting PGD_2 binding to CRTH2 (using cells transfected with human or mouse CRTH2) are: murine CRTH2, 3.7 nM IC_{50}, human CRTH2, 4.5 nM. The IC_{50} values for Cmpd A inhibiting other prostenoid, thromboxane or cysteinyl leukotriene receptors DP1, BLT1, CysLT1, CysLT2, EP1, EP2, EP3, EP4, FP, IP and TP are all >10 μM. Additionally, Cmpd A displayed no activity on a full panel of G protein-coupled receptors as determined by a PanLabs screen (MDS

Pharma, King of Prussia, PA, USA). The ED_{50} of Cmpd A in FITC-induced ear swelling assays was calculated to be 0.13 mg kg^{-1}. Taken together, this biological profile of Cmpd A demonstrates that it is a highly potent and selective CRTH2 antagonist (19).

FITC-induced contact hypersensitivity

A 1-week acute model of FITC-induced allergic inflammation was carried out as follows. The bellies of female BALB/c mice were shaved on day 1 and on days 1 and 2 and 400 μl of a 0.5% FITC solution was painted on the shaved ventral skin (dissolved in acetone:dibutyl phthalate, 1:1, v/v). Six days later, the mice were challenged with 0.5% FITC on the right ear (20 μl volume) or FITC vehicle (Veh) only on the left ear (20 μl volume). The Veh/veh cohort received the FITC Veh for the sensitization on days 1 and 2 and Veh on both ears for challenge. Mice were orally dosed with drug Veh, Cmpd A or ramatroban 1 h before challenge. For experiments that lasted >8 h, mice were dosed again at 7 h post-challenge. Dexamethasone (Dex) (5 mg kg^{-1}) was dissolved in PBS and administered intra-peritoneally at the same time points as the orally dosed drugs. Ear thickness of both ears was determined at set time points after the FITC challenge using a Digital Calipers (Fisher Scientific, Pittsburgh, PA, USA). The thickness of the left ear after FITC Veh challenge was almost identical to values prior to challenge from the first time point measured, 4 h (Stefen A. Boehme, unpublished observations). In some experiments, mice were treated with an anti-murine TSLP-neutralizing antibody (500 μg per mouse injected intravenously 1 h prior to FITC challenge; clone 152614, R&D Systems, Minneapolis, MN, USA) or an isotype-matched control antibody (rat IgG2A, R&D Systems). Ear edema, or change in ear thickness (Δ ear thickness), was expressed by thickness of the right (FITC-challenged ear) − thickness of the left ear, unless otherwise noted.

Analysis of cytokine and chemokine levels in challenged ears

After measuring ear thickness, mice were sacrificed and the ears were snap frozen in a dry ice/liquid nitrogen bath and stored at −80°C until analysis. Ears were then immersed in T-PER protein isolation buffer (Pierce, Rockford, IL, USA), containing freshly added protease and phosphatase inhibitors, and homogenized using an IKA ULTRA-TURRAX homogenizer (IKA Works, Inc., Wilmington, NC, USA). Solid contaminants (e.g. hair) were removed by centrifugation at 4°C, and the protein levels in the supernatant were quantitated by a BCA Protein Quantitation Assay (Pierce). Cytokine or chemokine levels in the protein lysates were assessed by ELISA analysis, and 50 or 100 μg of protein were used per data point. Each ear was homogenized and had protein levels determined independently. ELISAs were carried out on each individual sample (mouse ear) separately, and each sample was analyzed in triplicate or duplicate. The average of all the samples from an experimental group ± standard error of the mean (SEM) is shown. All ELISA kits were purchased from R&D Systems, with the exception of IL-4, which was obtained from BD PharMingen (San Diego, CA, USA). All ELISAs were used according to the manufacturer's protocol.

Gene expression analysis

The right and left ears were snap frozen in a dry ice/liquid nitrogen bath and stored at −80°C until RNA isolation. Total RNA was isolated using the Oligotex RNA Isolation Kit according to manufacturer's directions (Qiagen Sciences, Valencia, CA, USA). Biotinylated complementary RNA was prepared using the Illumina RNA Amplification Kit according to the manufacturer's instructions (Ambion, Inc., Austin, TX, USA). Messenger RNA (mRNA) was converted to cDNA and then amplified and labeled by T7 DNA polymerase. The Illumina Mouse 6 Sentrix Expression BeadChip was used (Illumina, San Diego, CA, USA). Following hybridization and washing, the arrays were scanned on an Illumina BeadArray Reader. The signals were computed with weighted averages of pixel intensities and local background was subtracted. Sequence-type signal was calculated by averaging corresponding bead signals from the three liver samples with outliers removed (median absolute deviation).

Simultaneous normalization of multiple microarrays was done using the 'mloess' method (20). Genes were ranked according to interest. In designing the interest statistic, we borrow ideas from Cole *et al.* (21) and their software package Focus. The interest statistic reflects a biologist's view that a gene with a greater fold change (in absolute value) than other genes is potentially the more interesting one. Also, given two genes with the same fold changes, it is the gene with a higher expression level (and therefore higher absolute change) that is the more interesting one. Genes were subsequently organized into functional groups and their expression patterns displayed as a heatmap.

Array data have been deposited in the EBI Array Express Database (accession number is pending).

Quantitative real-time PCR analysis

Relative mRNA transcript levels were measured by real-time quantitative reverse transcription (RT)–PCR in a LightCycler 480 (Roche Applied Science, Pleasanton, CA, USA). Total RNA was reverse transcribed using the Roche Transcriptor Kit and 50 ng cDNA were quantified using LightCycler 480 Probe Master Kit (Roche Applied Science). Duplicate biological samples were used. Each sample was run as a technical duplicate and mean values were reported. Normalized gene expression values were obtained using LightCycler Relative Quantification software. Relative gene copy numbers were derived by efficiency-corrected relative quantification using the formula $2^{\Delta CT}$, where ΔCT is the difference in amplification cycles required to detect amplification product from equal starting concentrations of RNA. The sequences of the oligonucleotide primers and the corresponding Universal Probe Library probe were supplied by Roche Applied Science. Results were expressed as fold change compared with the Veh/veh-treated animals.

Histological analysis

For histological examination, ear specimens were fixed in 10% buffered formalin and embedded in paraffin. Four-micron sections were stained with hematoxylin and eosin (H and E). For immunohistochemistry, ears were frozen in OCT medium (Tissue Tech, Torrance, CA, USA) in a dry ice/

isopentane bath. Ears were subsequently sectioned and stained with rat–anti-mouse GR-1 (clone RB6-8C5, BD Phar-Mingen) followed by an anti-rat antibody conjugated to alkaline phosphate and coverslipped using Vectashield Mounting Medium (Vector Laboratories, Burlingame, CA, USA). Human skin was obtained by surgical removal from healthy, control patients after written consent and approval by the local ethics committee. The human skin was frozen in OCT, sectioned and stained with a rabbit anti-human CRTH2 polyclonal antibody (Cayman Chemical). An anti-rabbit antibody conjugated to HRP was used for visualization of CRTH2. Control sections were stained with either a non-antigen-specific rabbit polyclonal primary antibody followed by the secondary antibody or the secondary antibody alone. All slides were imaged using a Zeiss Primostar microscope (Zeiss MicroImaging, Thornwood, NY, USA), a Moticam 2000 camera Motic Images Plus 2.0 software (Motic, British Columbia, Canada).

Statistics

The data are presented as the mean values ± SEM, unless stated otherwise. Statistical differences between data sets were analyzed by one-way analysis of variance and differences between groups were determined by Student's *t*-test. Statistics were computed by GraphPad Instat 3 software (GraphPad Software, San Diego, CA, USA). *P* values <0.05 were considered statistically significant.

Results

CRTH2 antagonist blocks FITC-induced ear swelling

To examine the role of the CRTH2 receptor in cutaneous inflammation, we used an allergic contact dermatitis model in which mice are sensitized to FITC on days 1 and 2 and 6 days later are challenged by FITC application to the right ear. The left ear serves as a control because it is treated with an equal amount of the FITC Veh (acetone:dibutyl phthalate). This experimental system has similarities to AD in humans, as it is CD4^{+} T lymphocyte dependent, and much of the pathology seen is analogous to acute AD lesions (11, 22). We first investigated whether the administration of a specific, potent CRTH2 antagonist, Cmpd A, could block the edema induced by FITC at the 24-h time point (Cmpd A is described in the Materials and methods, ref. 19). As comparators, we also tested ramatroban, a thromboxane A2 receptor antagonist that weakly cross-reacts with CRTH2 (23), the DP1 antagonist BW868c and Dex. As shown in Fig. 1(A), Cmpd A reduced ear swelling by ~85%; Dex and ramatroban were slightly less potent. BW868c had no effect, indicating that CRTH2 is the PGD_2 receptor mediating this response. Histological analysis showed that FITC/veh mice had profuse leukocyte infiltrates with both dermal and epidermal infiltration (Fig. 1B). Cell types contained in this infiltrate included lymphocytes, eosinophils and to a lesser extent neutrophils. Foci of microabscesses were observed in the epidermis, and the pustules, which were commonly seen in the acute and subacute dermatitis, contained lymphocytes, eosinophils and monocytes/macrophages as revealed by immunohistochemistry (IHC) analysis (data not shown). These
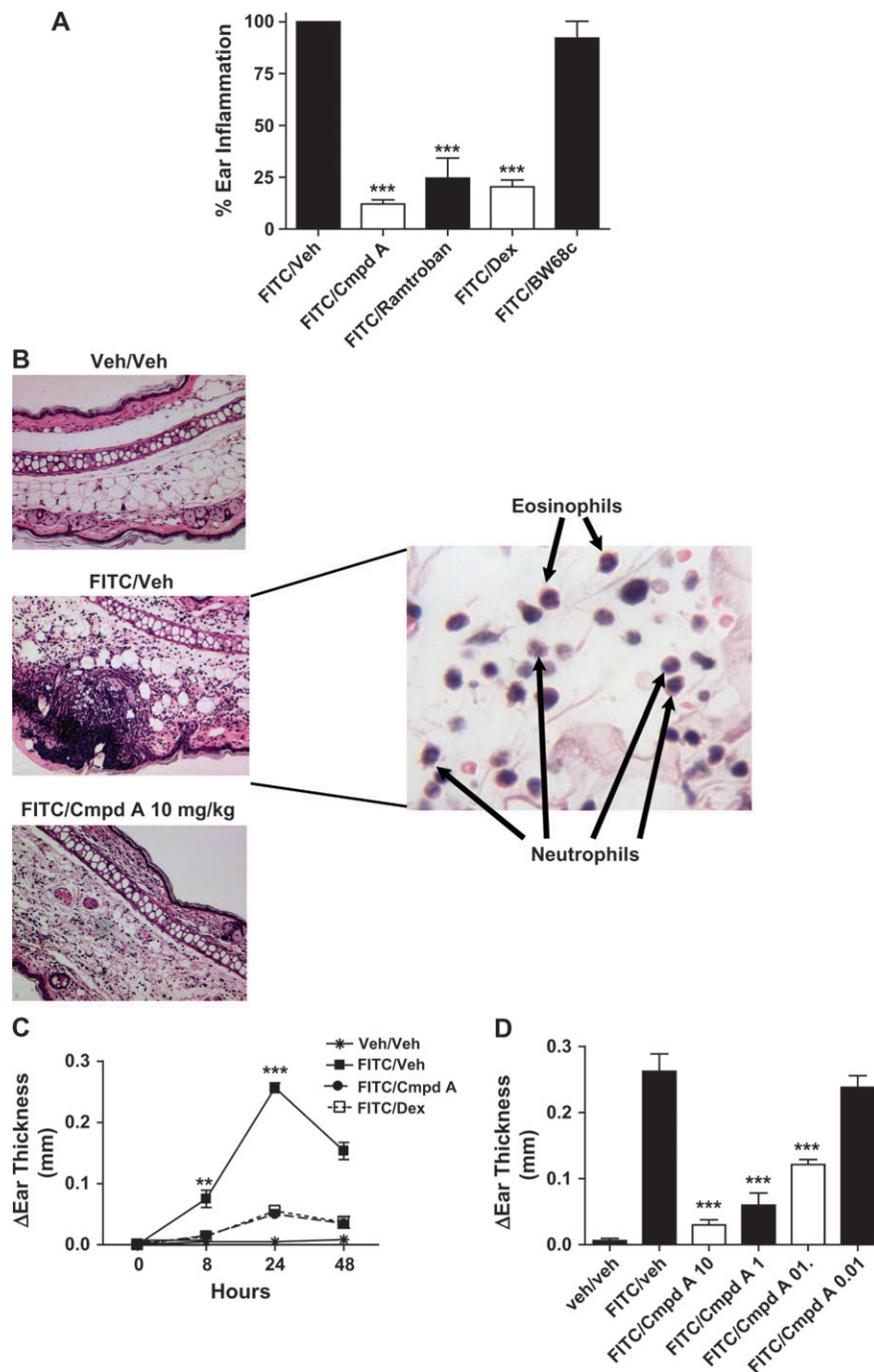
Fig. 1. The CRTH2 antagonist, Cmpd A, inhibits FITC-induced ear swelling in an allergic contact inflammation model. (A) One hour prior to ear challenge, the mice were dosed as follows, FITC/veh group—drug Veh delivered orally (p.o.), FITC/Cmpd A—10 mg kg^{-1} Cmpd A delivered p.o. (Cmpd A is described in the Materials and methods, ref. 19), FITC/ramatroban—15 mg kg^{-1} ramatroban p.o., FITC/Dex—Dex 5 mg kg^{-1} delivered intra-peritoneally (i.p.) and FITC/BW868c—15 mg kg^{-1} BW868c intravenously. Seven hours after challenge, the mice were dosed a second time. After 24 h, the thickness of both ears was measured using Digital Calipers. Ear edema was determined by subtracting the width of left ear (Veh treated) from the right ear (FITC treated) width. The thickness of the left ear (Veh challenged) after 24 h is almost identical to the untreated ear thickness. In this experiment, the percentage of ear inflammation was determined by comparing the ear edema from individual animals of the different treatment groups to the average change in right ear thickness of the FITC/veh group, which was set to 100%. (B) Histological analysis of H and E-stained right ear sections 24 h after FITC challenge. Inset is FITC/veh at high power ($\times$100) showing eosinophils and neutrophils in the inflammatory infiltrate. (C) Kinetic analysis of FITC-induced ear swelling showing peak edema at 24 h and partial resolution at 48 h post-challenge. The Veh/veh group and FITC/Veh group were received with drug Veh, the FITC/Cmpd A cohort was administered 10 mg kg^{-1} of Cmpd A p.o. and the FITC/Dex received 5 mg kg^{-1} Dex i.p. All groups were treated 1 h prior to FITC challenge and 7 h post-ear challenge. The average change in ear thickness per group is shown $\pm$ SEM. (D) Cmpd A inhibits FITC-induced ear edema in a dose-dependent manner. Mice were treated with the described dose of Cmpd A or drug Veh 1 h prior to FITC ear challenge and 7 h after challenge. At 24 h, ear thickness was measured, and the change in thickness of the challenged (right) ear is shown $\pm$ SEM. For all experiments shown, a minimum of five animals were used per treatment group, and ***$P < 0.001$, **$P < 0.01$.

histological features are similar to the acute manifestation of a late-phase IgE-dependent allergic reaction commonly found in AD patients (24). Mice treated with Cmpd A at the time of FITC ear challenge showed substantially less infiltration of mononuclear cells, including lymphocytes, eosinophils and neutrophils, and no epidermal microabscesses. This underscores the critical role CRTH2 plays in the inflammatory response as a whole and in the formation of cutaneous lesions. As the administration of Cmpd A could conceivably change the kinetics of ear swelling in response to FITC challenge, we examined the response over time (Fig. 1C). In the FITC/veh-treated animals, the inflammatory reaction peaked at 24 h, consistent with results reported by other groups (11). Both Cmpd A- and Dex-treated animals displayed greatly diminished ear swelling at all the time points measured, 8, 24 and 48 h. Dose–response analysis was performed using the specific CRTH2 antagonist Cmpd A. As shown in Fig. 1(D), inhibition of FITC-induced ear swelling was reduced in a dose-dependent manner, with the 10 mg kg^{-1} dose showing the greatest efficacy, followed by the 1 and 0.1 mg kg^{-1} doses. Collectively, these data demonstrated that a specific CRTH2 antagonist can effectively inhibit FITC-induced edema and the accompanying cutaneous pathology in this acute model of contact hypersensitivity.

The CRTH2 antagonist, Cmpd A, modulated gene expression patterns in FITC-challenged mice

In an effort to understand how Cmpd A was inhibiting ear swelling following the application of FITC, mice were Veh challenged (Veh/veh), FITC challenged and drug Veh treated (FITC/veh), FITC challenged and Cmpd A treated (FITC/Cmpd A) and, as a control, FITC challenged and Dex treated (FITC/Dex) and ears were harvested at 4, 8 and 24 h post-FITC challenge. RNA was extracted for gene expression analysis between the different treatment groups at the various time points. A large number of cytokine and chemokine genes were up-regulated in FITC/veh-treated animals, particularly at 8 h post-challenge (Fig. 2A). This appeared to coincide with the inflammatory time course, as the increased swelling detected at the 24-h time point followed the increased transcription of pro-inflammatory cytokine and chemokine genes at 8 h. An examination of the Cmpd A-treated mice showed a dramatic decrease in RNA levels compared with the drug Veh-treated cohort. In particular, the pro-inflammatory cytokines such as IL-1β, IL-4 and IL-13 are down-regulated by Cmpd A treatment, as are the chemokines CCL7/MCP-3, CCL4/MIP-1β and CXCL9/MIG. The expression of atopy-associated genes mucin-1 and trefoil factors 1, 2 and 3 (tff 1, 2 and 3) are also down-regulated in Cmpd A-treated animals compared with drug Veh-treated mice (Fig. 2B). A number of genes that have been genetically linked to atopic diseases are also up-regulated by FITC treatment and have decreased expression upon Cmpd A treatment (25). Some of these genes include small proline-rich protein 2A, calgranulin A and B and PHD finger protein 11 (Fig. 2C). Quantitative PCR (qPCR) analysis confirms the decrease of calgranulin B/S100 calcium-binding protein A9 observed with the microarray analysis (Fig. 2D). It should be noted that leukotriene receptors LTB$_4$ R1 and R2 are up-regulated by FITC challenge and Cmpd A treatment results

in decreased RNA levels, similar to other genes in the arachidonic acid pathway cluster. Thus, blockade of the PGD$_2$–CRTH2 interaction inhibits the up-regulation of a broad array of pro-inflammatory genes. It is also noteworthy that quite a few genes, particularly in the CC chemokine, cytokine and arachidonic acid pathway clusters, were strongly up-regulated 24 h post-FITC challenge in the Dex treatment group (FITC/Dex) in contrast to the Cmpd A-treated animals.

Effect of Cmpd A on cytokine protein levels from FITC-challenged ears

We next wanted to confirm and extend the findings observed with the microarray and qPCR analysis by analyzing protein lysates made from challenged ears. Kinetic analysis of IL-4 protein expression was consistent with the RNA analysis, as IL-4 protein levels were significantly reduced at the 8-, 24- and 48-h time points in the FITC–Cmpd A-treated mice (Fig. 3A). IL-4 levels in the Dex-treated mice were also strongly down-regulated, in line with its inhibitory effect on the NF-AT transcription factor. Kinetic analysis of IFN-γ protein amounts demonstrated that Cmpd A reduced levels at 8 h compared with the FITC/veh cohort, but at the 24- and 48-h time points the suppressive effect disappeared (Fig. 3B). Dex had no significant effect on IFN-γ protein levels. We next examined the effect of Cmpd A on the protein levels of two pro-inflammatory cytokines previously shown to play a role in cutaneous inflammation, TNF-α and transforming growth factor-β (TGF-β) at 24 h post-challenge (11, 26). TNF-α protein levels are strongly reduced by the two doses of Cmpd A examined (Fig. 3C). Similarly, Cmpd A reduced the levels of TGF-β, however, not to the same level as Dex treatment (Fig. 3D). These experiments importantly demonstrate that the oral administration of the CRTH2 antagonist Cmpd A effectively reduced the levels of a number of key pro-inflammatory cytokines produced locally at the site of inflammation.

Cmpd A reduced the levels of the CXC chemokines MIP-2 and GRO-α

A dermal neutrophilic infiltrate has previously been shown in both human acute AD lesions, as well as this FITC model of allergic cutaneous inflammation (22, 24). Furthermore, other critical cell types in addition to CD4$^+$ T lymphocytes involved mediating allergic contact dermatitis include dermis-localized mast cells and epithelial cells including keratinocytes. These three cell types are capable of producing either or both the CXC chemokines MIP-2 (CXCL2), the functional analog of human IL-8, and GRO-α (CXCL1, ref. 27). Both these chemokines have the ability to recruit neutrophils to sites of skin inflammation (28). We wanted to investigate whether blocking CRTH2 would impact the production of these CXC chemokines and the subsequent neutrophil influx. Mice were administered Cmpd A 1 h prior to FITC ear challenge, and GRO-α and MIP-2 protein levels were measured at 8 and 24 h. Cmpd A had little effect on the chemokine levels at 8 h; however, there was a significant decrease in both MIP-2 and GRO-α protein at 24 h (Fig. 4A and B). Challenged ears from mice of the same cohort were isolated at 24 h and stained for the expression of GR-1 (Ly-6G), a glycosyl-phosphatidylinositol-linked protein
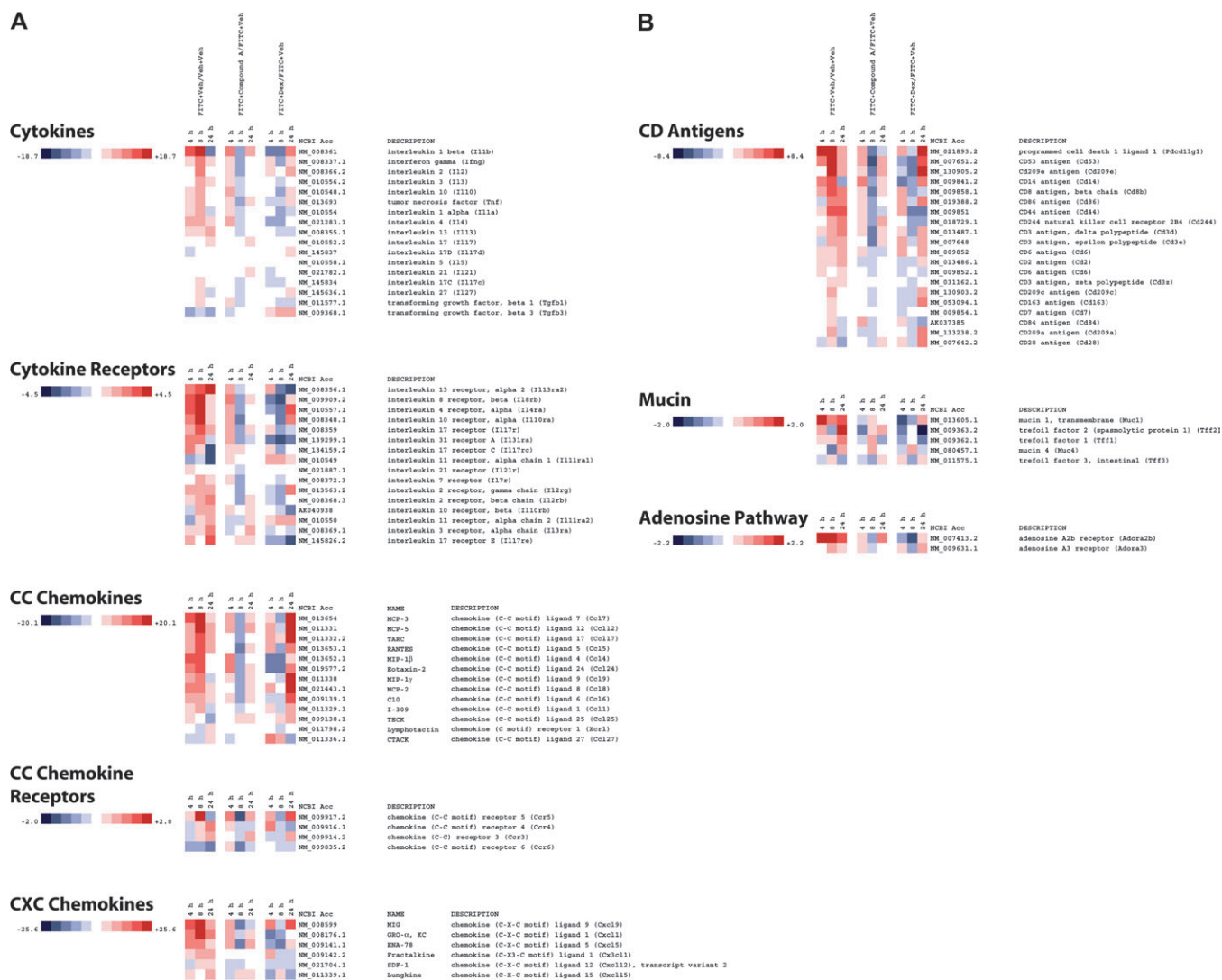
A

B

Fig. 2. Heatmap of select genes down-regulated in FITC-challenged ears treated with Cmpd A at 4, 8 and 24 h. Total RNA was extracted and analyzed using Illumina BeadArrays. Levels of gene expression were investigated in four treatment groups at 4-, 8- and 24-h time points using Illumina BeadArrays. The groups included Veh-treated animals (Veh on both ears and oral administration of drug Veh alone, Veh/veh), challenged animals/drug Veh (right ear challenged with FITC, left ear with Veh; oral administration of drug Veh only, FITC/veh), challenged animals/Cmpd A treated (right ear challenged with FITC, left ear with Veh; oral administration of Cmpd A 10 mg kg^{-1}, FITC/Cmpd A) and challenged animals/ Dex (right ear challenged with FITC, left ear with Veh; intra-peritoneal administration of Dex 5 mg kg^{-1}, FITC/Dex). The array data are representative of three independent experiments (biological replicates). The fold changes are noted on the respective color scales. In the clustergrams, genes are grouped into (A) cytokines, cytokine receptors, CC chemokines, CC chemokine receptors and CXC chemokines. (B) CD antigens, mucin cluster and adenosine pathway. (C) arachidonic acid pathway, signaling molecules and transcription factors. (D) Levels of S100 calcium-binding protein A9 (calgranulin B) (S100a9), as determined by RT–qPCR. The data were normalized relative to β-actin and are presented as fold increases or decreases between FITC + Veh/veh, FITC + Cmpd A/FITC and FITC + Dex/FITC-treated mice. The RT–qPCR is representative of two independent experiments (biological replicates) performed in duplicate.
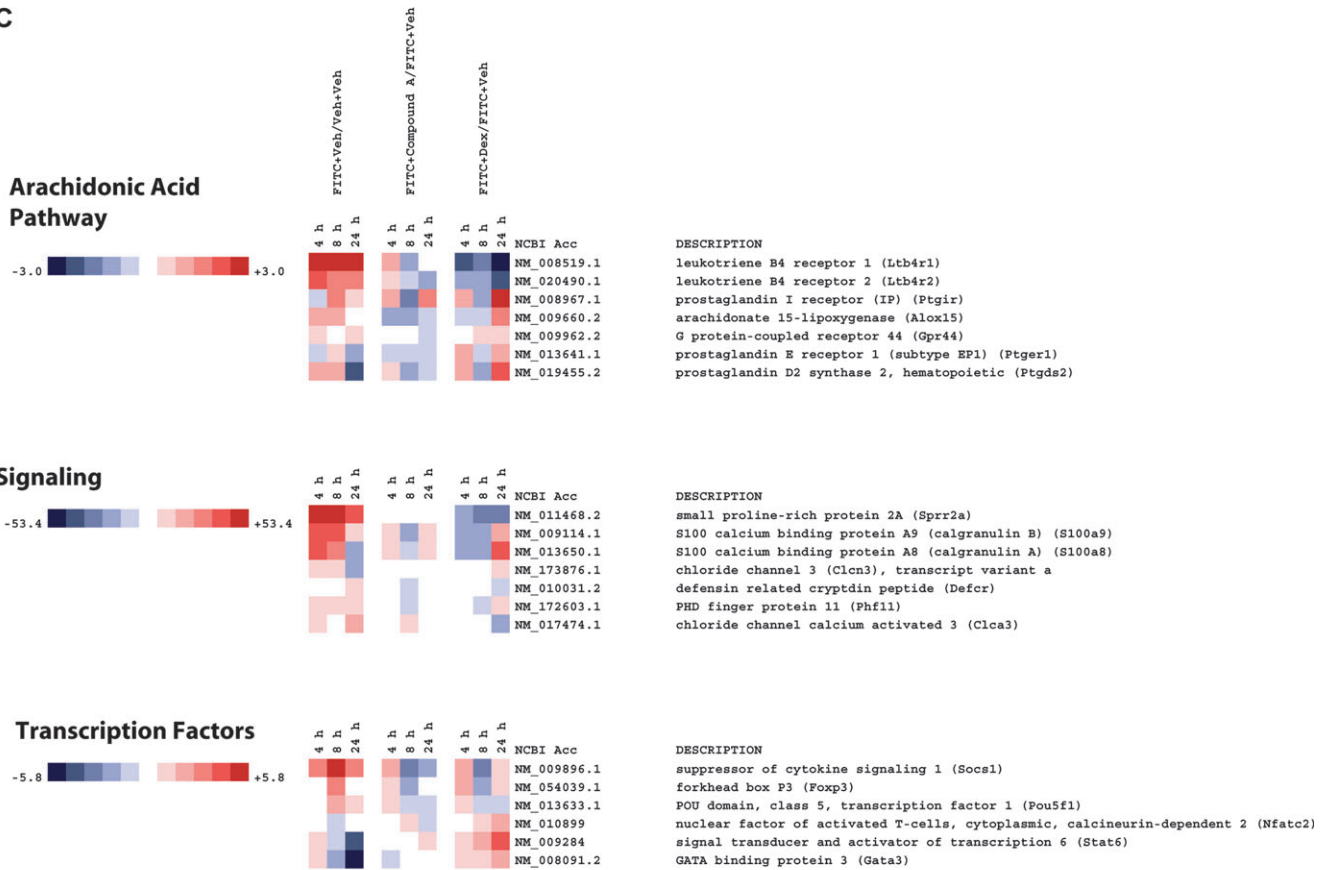
expressed by neutrophils in the periphery, and on eosinophils, albeit at lower cell surface levels. As seen in Fig. 4(C), there was a dramatic decrease in GR-1$^+$ cells upon Cmpd A treatment, consistent with the decrease in GRO-α and MIP-2. This striking inhibition of GR-1$^+$ neutrophil and eosinophil influx would certainly be expected to account for at least some of the decrease in ear edema observed by the administration of Cmpd A. Thus, Cmpd A had a strong effect inhibiting the production of the neutrophil chemoattractants GRO-α and MIP-2 and the influx of neutrophils, the latter being a feature often found in the acute

lesions of AD patients. These results also demonstrated that the CRTH2 antagonist impacted the recruitment of cell types that do not express CRTH2.

IL-1β and TSLP protein levels are reduced by Cmpd A

Cytokines expressed in the early stages of an allergic contact dermatitis reaction would be expected to play a key role in orchestrating downstream inflammation. Gene expression analysis showed that pro-inflammatory cytokine IL-1β is induced ~15-fold 4 h after FITC challenge (Fig. 2A), and its levels are decreased by Cmpd A. Further, epithelial cells

C

Arachidonic Acid Pathway

−3.0 ▮▮▮▮ ▮▮▮▮ +3.0

	FITC+Veh/Veh+Veh			FITC+Compound A/FITC+Veh			FITC+Dex/FITC+Veh				
	4 h	8 h	24 h	4 h	8 h	24 h	4 h	8 h	24 h	NCBI Acc	DESCRIPTION
										NM_008519.1	leukotriene B4 receptor 1 (Ltb4r1)
										NM_020490.1	leukotriene B4 receptor 2 (Ltb4r2)
										NM_008967.1	prostaglandin I receptor (IP) (Ptgir)
										NM_009660.2	arachidonate 15-lipoxygenase (Alox15)
										NM_009962.2	G protein-coupled receptor 44 (Gpr44)
										NM_013641.1	prostaglandin E receptor 1 (subtype EP1) (Ptger1)
										NM_019455.2	prostaglandin D2 synthase 2, hematopoietic (Ptgds2)

Signaling

−53.4 ▮▮▮▮ ▮▮▮▮ +53.4

	4 h	8 h	24 h	4 h	8 h	24 h	4 h	8 h	24 h	NCBI Acc	DESCRIPTION
										NM_011468.2	small proline-rich protein 2A (Sprr2a)
										NM_009114.1	S100 calcium binding protein A9 (calgranulin B) (S100a9)
										NM_013650.1	S100 calcium binding protein A8 (calgranulin A) (S100a8)
										NM_173876.1	chloride channel 3 (Clcn3), transcript variant a
										NM_010031.2	defensin related cryptdin peptide (Defcr)
										NM_172603.1	PHD finger protein 11 (Phf11)
										NM_017474.1	chloride channel calcium activated 3 (Clca3)

Transcription Factors

−5.8 ▮▮▮▮ ▮▮▮▮ +5.8

	4 h	8 h	24 h	4 h	8 h	24 h	4 h	8 h	24 h	NCBI Acc	DESCRIPTION
										NM_009896.1	suppressor of cytokine signaling 1 (Socs1)
										NM_054039.1	forkhead box P3 (Foxp3)
										NM_013633.1	POU domain, class 5, transcription factor 1 (Pou5f1)
										NM_010899	nuclear factor of activated T-cells, cytoplasmic, calcineurin-dependent 2 (Nfatc2)
										NM_009284	signal transducer and activator of transcription 6 (Stat6)
										NM_008091.2	GATA binding protein 3 (Gata3)

D

S100a9

Legend: 4 hrs / 8 hrs / 24 hrs

Y-axis: Ratio relative to Veh/veh (0–40)

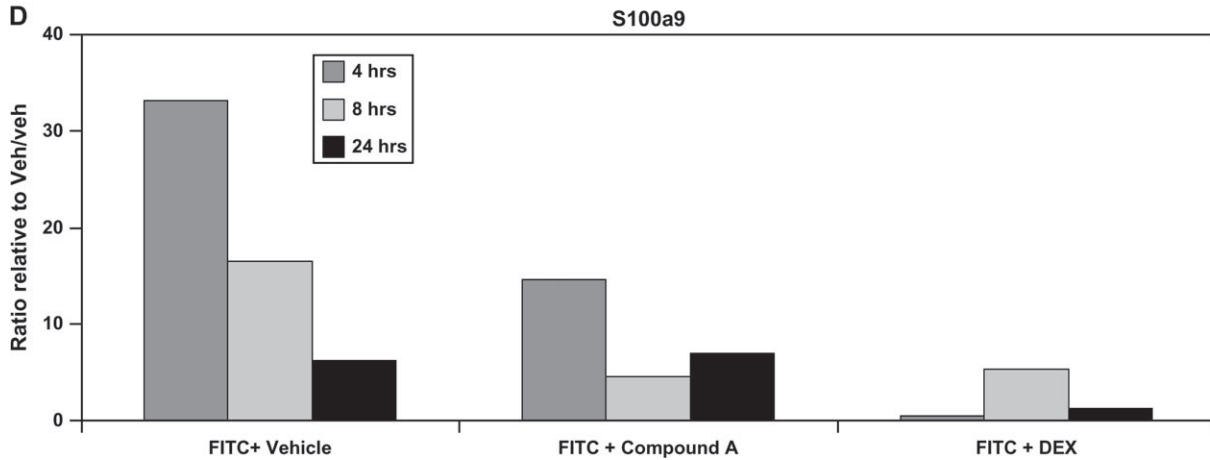X-axis categories: FITC+ Vehicle, FITC + Compound A, FITC + DEX

Fig. 2. continued.

and keratinocytes can express IL-1β. An examination of IL-1β in ear lysates show that Cmpd A protein levels are reduced by ~33% at the 4-h time point (Fig. 5A).

Another cytokine that is rapidly released by epithelial cells in response to a wide range of stimuli, including IL-1, is TSLP. We examined the production of TSLP because (i) it is over-expressed in AD lesions (29), (ii) has the ability to elicit IL-4 production from murine CD4⁺ T lymphocytes (30, 31) and (iii) can prime skin-residing dendritic cells for activation and migration to draining lymph nodes upon antigen capture (4).

Four hours after FITC or Veh challenge, ears were assayed for TSLP protein levels. Interestingly, we noticed there was a large amount of TSLP present in the Veh/veh-treated extracts that suggested that the acetone:dibutyl phthalate mixture could induce TSLP production (Fig. 5B). Nevertheless, topical application of FITC resulted in a 2-fold increase in TSLP over Veh/veh levels, and Cmpd A reduced TSLP to similar levels as the Veh/veh-treated animals. To investigate the induction of TSLP in Veh-treated mice, the Veh control left ears were also assayed for TSLP.
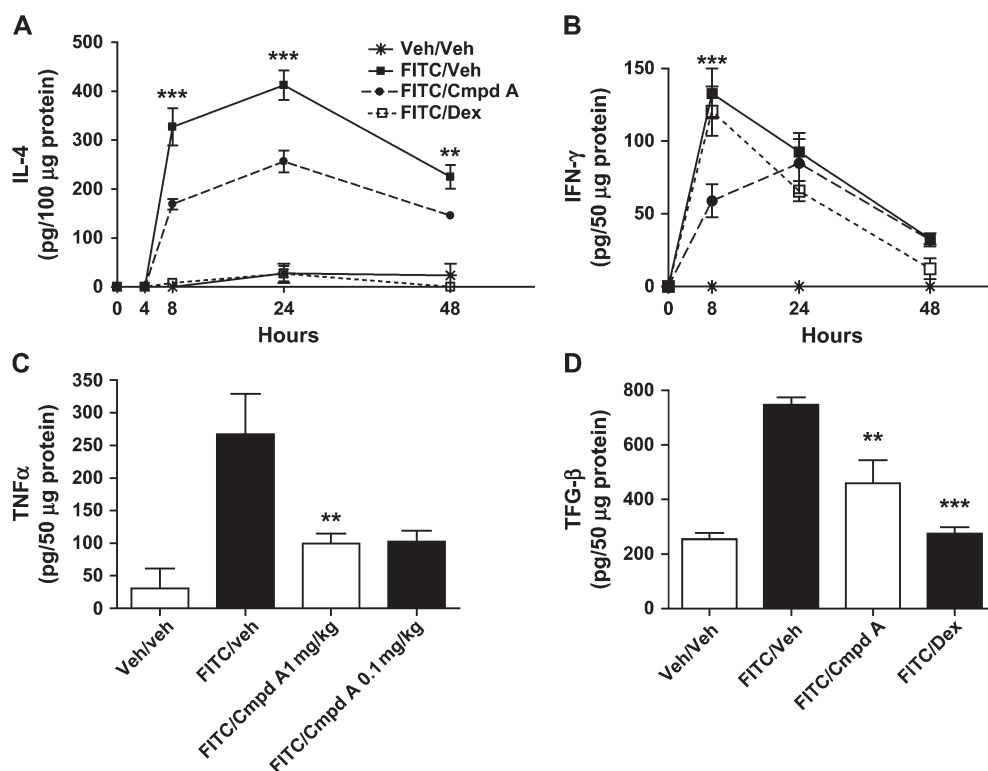
Fig. 3. Oral administration of Cmpd A reduces pro-inflammatory cytokine levels in FITC-challenged ears. Protein lysates from ears were examined for cytokines by ELISA analysis. Right and left ears were harvested from mice at the indicated time points (4, 8, 24 and 48 h) for IL-4 (A); 8, 24 and 48 h for IFN-γ (B); and 24 h for TNF-α (C) and TGF-β (D). Each point shown represents the average cytokine value ($\pm$SEM) from a minimum of five mice, and each lysate was tested independently in duplicate or triplicate as described in the Materials and methods. Mice were treated in the following conditions in panels (A, B and D): Veh challenged on the right and left ear and drug Veh administered p.o. (Veh/veh), FITC challenged on the right ear, Veh on the left ear and drug Veh given p.o. (FITC/veh), FITC-challenged right ear, Veh-challenged left ear and Cmpd A (10 mg kg^{-1}) delivered p.o. (FITC/Cmpd A) and FITC-challenged right ear, Veh-challenged left ear and Dex (5 mg kg^{-1}) administered intraperitoneally (FITC/Dex). In panel (C), one Cmpd A treatment group received 1 mg kg^{-1} and another 0.1 mg kg^{-1}, as labeled. Values expressed as petagram per 50 μg of total protein, except for IL-4 which is expressed as petagram per 100 μg total protein. There were a minimum of five mice per treatment group. ***$P < 0.001$, **$P < 0.01$.

Interestingly, there was a 3- to 4-fold induction of TSLP in ears challenged with just acetone:dibutyl phthalate compared with a naive ear (Fig. 5C). There was also no significant difference in the TSLP levels from control ears of mice treated with drug Veh or Cmpd A, demonstrating that the CRTH2 antagonist effect on TSLP production was limited to allergen challenge. Finally, there was no detectable IL-1β or TSLP 1 h post-FITC challenge (data not shown).

Anti-TSLP can modulate FITC-induced ear swelling and cytokine production

We next used an anti-TSLP-neutralizing mAb to investigate the role of TSLP in this acute allergic dermatitis model in greater depth. Mice were first sensitized to FITC and 6 days later were treated with Cmpd A (1 mg kg^{-1}), a suboptimal dose of Cmpd A (0.1 mg kg^{-1}) plus an isotype-matched antibody, an anti-TSLP antibody and anti-TSLP antibody together with 0.1 mg kg^{-1} Cmpd A. Twenty-four hours after FITC challenge, ear swelling was assessed, and the ears were then harvested for histological analysis and cytokine production. In this experiment, 1 mg kg^{-1} of Cmpd A reduced ear swelling $\sim$70%, and the 0.1 mg kg^{-1} dose was expectedly less efficacious ($\sim$30% reduction) (Fig. 6A).

A similar reduction in ear swelling was seen in the anti-TSLP-treated mice ($\sim$30%). However, the co-administration of 0.1 mg kg^{-1} Cmpd A and anti-TSLP reduced the inflammation to levels observed with the 1 mg kg^{-1} Cmpd A treatment. This synergistic effect between Cmpd A and anti-TSLP suggested that multiple pathways lead to allergic inflammation and skin lesions and that TSLP played only a partial role. In contrast, the amelioration of ear swelling and reduction of TSLP by Cmpd A suggests that the CRTH2 antagonist can inhibit multiple pathways leading to allergic inflammation in this acute model of contact dermatitis. H and E analysis of ear sections shows a large inflammatory infiltrate and pustule formation from animals treated with drug Veh, 0.1 mg kg^{-1} Cmpd A and anti-TSLP (Fig. 6B). Animals receiving 1 mg kg^{-1} Cmpd A and both anti-TSLP together with 0.1 mg kg^{-1} Cmpd A had a decreased inflammatory infiltrate. An examination of IL-4 levels showed an $\sim$40% decrease upon 1 mg kg^{-1} Cmpd A treatment (Fig. 6C). Similar to the ear swelling, both suboptimal levels of Cmpd A or anti-TSLP treatment reduced IL-4 to an intermediate level, and the combination of both resulted in a decrease comparable to the 1 mg kg^{-1} dose of Cmpd A. This suggests that IL-4 is being induced by both TSLP-dependent and independent pathways. Interestingly,
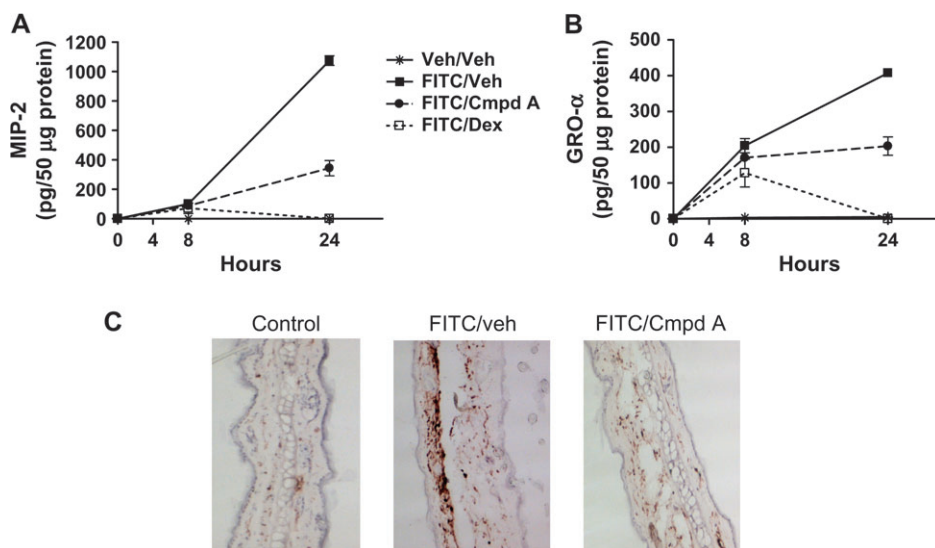
Fig. 4. Cmpd A reduces MIP-2 and GRO-α production and the recruitment of neutrophils (GR-1^{+} cells) in FITC-challenged ears. Protein lysates from challenged ears isolated at 8 and 24 h were assayed by ELISA for MIP-2 (A) and GRO-α (B) protein levels. Values shown are the petagram of cytokine measured from 50 μg total protein, and the average of five mice per treatment group ± SEM is shown, as detailed in the Materials and methods. The treatment groups are Veh/veh, FITC/veh, FITC/Cmpd A 10 mg kg^{-1} p.o. and FITC/Dex 5 mg kg^{-1} intra-peritoneally (C) IHC analysis of ears isolated at 24 h post-FITC challenge and stained with an anti-GR-1 mAb to label neutrophils.
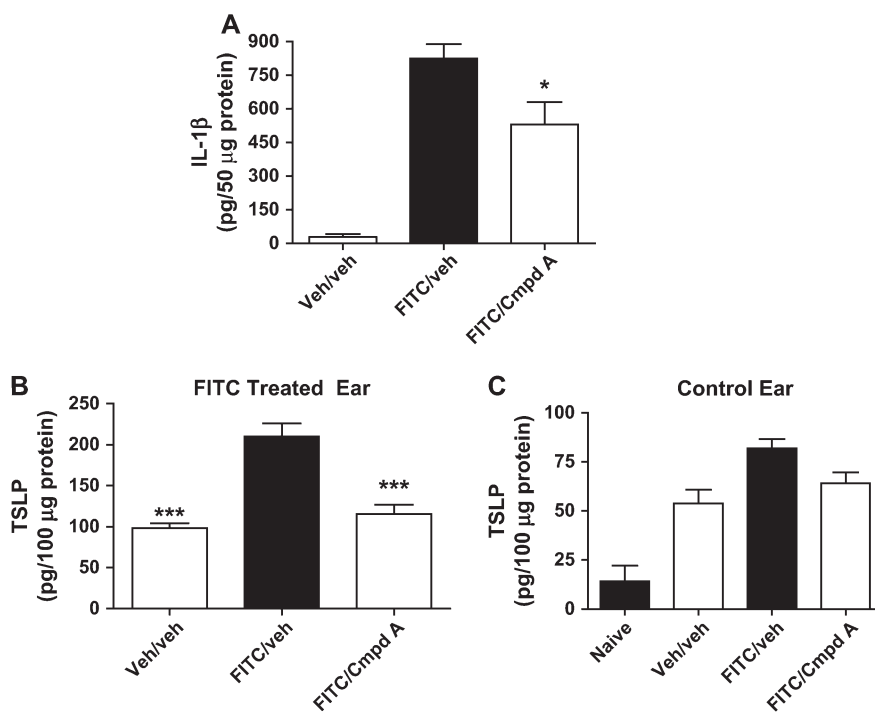
Fig. 5. IL-1β and TSLP protein levels are reduced 4 h after FITC challenge by Cmpd A. Mice were treated with either drug Veh or Cmpd A (1 mg kg^{-1}) 1 h before FITC challenge to the right ear. The left ears were challenged with FITC Veh (acetone:dibutyl phthalate). After 4 h, the ears were harvested and the protein lysates from the right ears were assayed for (A) IL-1β (50 μg total protein) and (B) TSLP (100 μg total protein). As TSLP levels were high in the Veh/veh group, the left ears (Veh challenged) from mice in all the groups were assayed for TSLP protein levels (C). Additionally, six ears from untreated BALB/c mice were also examined for TSLP protein levels. A minimum of five animals were tested per condition except where noted above, and the results show the mean ± SEM. ***$P < 0.001$, *$P < 0.05$.

anti-TSLP treatment had no effect on GRO-α levels in the ear, whereas both concentrations of Cmpd A tested brought levels down significantly (Fig. 6D). This further illustrates that multiple pathways are impacted by inhibition of the CRTH2–PGD$_2$ interaction that culminates in reducing FITC-induced inflammation.
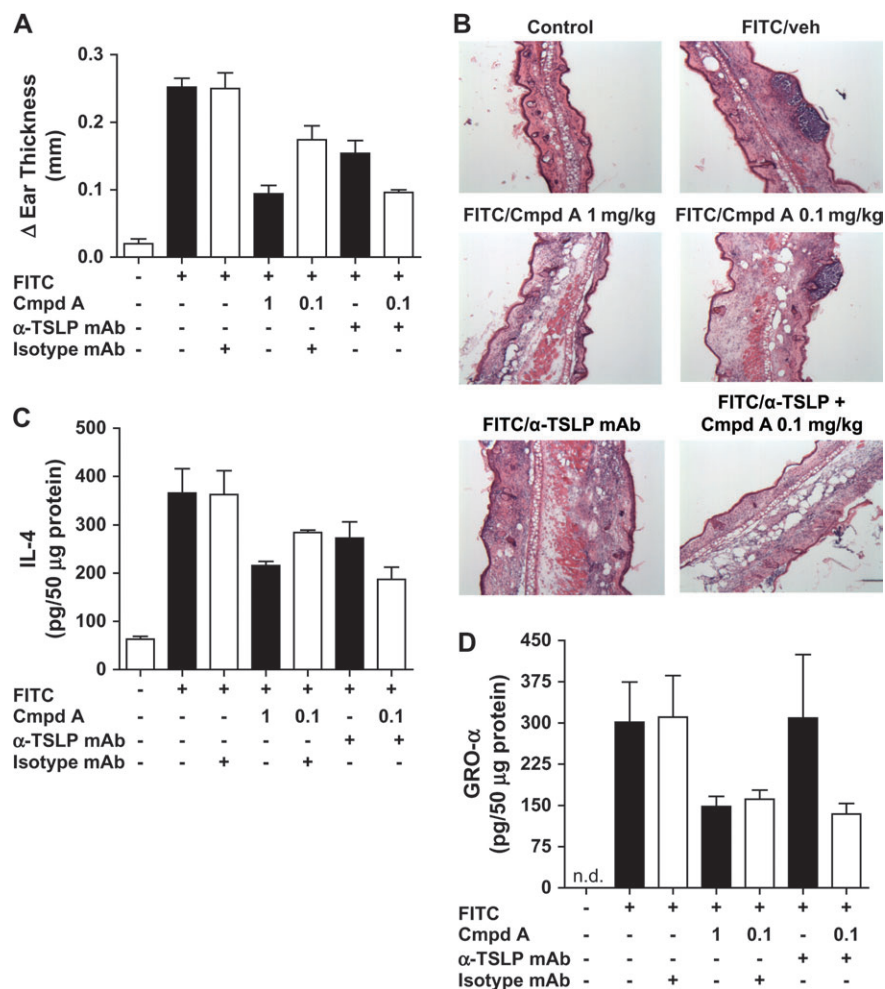
Fig. 6. Anti-TSLP antibody treatment only partially inhibits allergic inflammation in contrast to CRTH2 antagonism. One hour prior to FITC challenge, mice received drug Veh p.o., drug Veh p.o. and 500 µg control antibody intravenously (i.v.), Cmpd A (1 mg kg^{-1}) p.o., Cmpd A (0.1 mg kg^{-1}) and control antibody i.v., anti-TSLP antibody (500 µg) i.v. and Cmpd A (0.1 mg kg^{-1}) p.o. and anti-TSLP antibody i.v. Seven hours after FITC challenge to the right ear, the appropriate groups received either drug Veh or Cmpd A p.o. (A) Twenty-four hours after challenge, ear thickness was determined and the change in thickness calculated. (B) Ear sections isolated 24 h after FITC challenge were stained with H and E. Protein lysates from the treated ears were assayed for IL-4 (C) and GRO-α (D). Fifty micrograms of total protein from lysates were analyzed by ELISA. The results show the mean cytokine levels ± SEM of a minimum of five mice per treatment group.
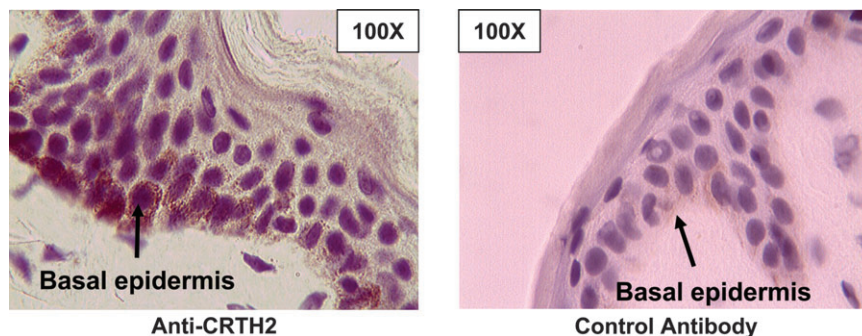

Fig. 7. CRTH2 is expressed by basal epidermal cells in human skin. Human skin was analyzed by IHC for CRTH2 expression using an anti-human CRTH2 polyclonal antibody (rabbit polyclonal). Control staining with a polyclonal rabbit primary antibody is also shown. No reliable anti-mouse CRTH2 antibody is available, so CRTH2 expression in mouse skin was not examined.

CRTH2 is expressed by the basal epidermal layer of human skin

Together, the induction of TSLP, IL-1β, GRO-α and MIP-2 expression suggested that cutaneous epithelial cells or keratinocytes may be directly or indirectly stimulated by PGD_2 released from activated mast cells, thereby initiating an allergic inflammatory response. To investigate this, human skin was examined by IHC analysis and revealed CRTH2 expression in the basal epidermis (Fig. 7). This observation raises the possibility that PGD_2 may initiate inflammation in this FITC model in part by activating CRTH2 expressed on epidermal cells.

Discussion

We used a well-characterized model of FITC-induced contact hypersensitivity to examine the role of the PGD_2 receptor, CRTH2, in mediating the inflammatory response. In this model, mice are sensitized to FITC by two topical applications to the ventral skin on days 1 and 2, and this results in FITC-specific IgE antibody production. Six days following the second abdominal painting, the mice are challenged by a topical FITC application to the right ear. The ensuing inflammatory response and skin lesions in many ways reflect acute lesions observed in human AD (11). Using this murine model, we established that much of the inflammatory response observed is dependent upon the CRTH2–PGD_2 receptor, and not on the DP1 receptor, as the DP1 antagonist, BW868c, did not inhibit ear swelling post-FITC challenge (Fig. 1A). Further, this response was both dose dependent and not due to delayed kinetics of the inflammation (Fig. 1C and D).

An investigation into the inflammatory mediators thought to play a role in orchestrating the inflammatory response proved insightful. One hour after challenge, we did not detect any IL-1β or TSLP in protein lysates from the FITC-treated ears (data not shown). However, 4 h post-challenge, both these mediators were readily detectable (Fig. 5). Interestingly, we noticed that the addition of the FITC Veh, acetone:dibutyl phthalate, induced TSLP in the absence of FITC. It has previously been noted that dibutyl phthalate has an adjuvant effect in this model of contact hypersensitivity and can increase trafficking of dendritic cells from the skin to the draining lymph nodes (32). Further, it has recently been shown that TSLP-treated epidermal Langerhans cells secrete increased amounts of the T_h2 T cell-attracting chemokine CCL17 (TARC) and promote the differentiation of naive $CD4^+$ T cells into pro-allergic T_h2 lineage T cells (33). The ability of dibutyl phthalate to act as an adjuvant may in part be attributable to our observation of its ability to induce TSLP production, thereby activating the skin dendritic cells (6) and Langerhans cells (33).

Investigating TSLP production in FITC-challenged ears showed that TSLP levels increase significantly over the levels observed with just Veh treatment. This increase upon FITC addition was almost completely abrogated by the oral administration of Cmpd A prior to challenge, suggesting that skin allergen-induced TSLP release was dependent upon CRTH2 activation, whereas the dibutyl phthalate-mediated TSLP production was not. The major producer of PGD_2 is activated mast cells, and these cells are present throughout the dermis and surrounding blood vessels. Because this model of contact hypersensitivity is both $CD4^+$ T cell and mast cell dependent (11), we hypothesized that IgE-mediated activation of mast cells, which results in the release of PGD_2, could directly stimulate keratinocytes or epithelial cells to produce TSLP. This, in turn, could initiate the inflammatory cascade consistent with the idea that TSLP is a 'master switch' for allergic inflammation (29). We also observed that human basal epidermal cells, and possibly keratinocytes which secrete TSLP (34), express the CRTH2 receptor (Fig. 7). To test whether CRTH2-mediated TSLP production was responsible for the allergic inflammation, we treated mice prior to ear challenge with a neutralizing anti-TSLP antibody in the presence or absence of a suboptimal dose of Cmpd A. No TSLP was detected in protein lysates of challenged ears from mice receiving the neutralizing antibody (data not shown). Together with the observation that anti-TSLP-treated animals displayed a reduced level of ear swelling, this suggested, but did not rule out, that TSLP was effectively neutralized. Animals that received the anti-TSLP antibody and the suboptimal dose of Cmpd A had a further reduction in ear swelling and a reduced inflammatory infiltrate. Additionally, levels of IL-4, a key pro-inflammatory cytokine in this model (11), were reduced to a greater degree by the combination of anti-TSLP and 0.1 mg kg^{-1} Cmpd A than either alone. This suggested that TSLP played a role in coordinating the inflammatory response to FITC challenge, but other non-TSLP-mediated pathways were also involved. This was confirmed by histological analysis, which showed a decreased inflammatory infiltrate in dually treated mice compared with mice that received either anti-TSLP antibody or 0.1 mg kg^{-1} Cmpd A alone, as well as the observation that anti-TSLP antibody treatment had no effect on GRO-α levels, but whose levels were greatly reduced by Cmpd A treatment (Figs 4 and 6B and D). These observations also suggest, although not directly tested, that PGD_2-mediated activation of CRTH2 may also positively regulate TSLP expression. Alternatively, PGD_2–CRTH2 may act via another rapidly induced cytokine, such as IL-1β.

Examining gene expression levels from FITC-challenged ears showed a dynamic pattern of up-regulation across many pro-inflammatory gene families. For instance, the transcription of many cytokines was dramatically increased within 4–8 h of FITC application and were negatively affected by Cmpd A, such as IL-4, IL-1α and β and IFN-γ. Similarly, many FITC-induced chemokines were negatively regulated by Cmpd A, including CCL7/MCP-3, CCL17/TARC, CCL5/RANTES, CCL24/eotaxin-2, CXCL9/MIG and CXCL1/GRO-α. There was no distinction of T_h1- or T_h2-type cytokines or chemokines being singularly modulated, and similarly, there is a wide array of cells including T and B cells, macrophages, eosinophils and neutrophils that could be stimulated by these cytokines and chemokines. Thus, consistent with the protein data, the gene expression analysis demonstrates that a wide range of inflammatory mediators are elicited by FITC challenge and are down-regulated by antagonism of CRTH2 via Cmpd A.

It is of interest to note that the major therapeutic effect seen with Cmpd A administration at the gene expression level occurred at 8 h with some (but not all) genes becoming

up-regulated again at 24 h. This may be a result of the predicted $T_{1/2}$ of Cmpd A being ~3 h in mice. Not all genes were back up, however, such as CCR4 and CCR6, the receptors for CCL17/TARC, CCL22/MDC and CCL20/MIP-3α, respectively, as well as a number of genes from other families, for example ALOX 15. While this may be reflective of the regulation specificities of the genes themselves, it is intriguing that in many examples, these same genes were rapidly and more strongly up-regulated at times later than 8 h following Dex treatment when compared with Cmpd A. This is particularly evident within the entire CC chemokine cluster of genes, suggesting that steroid treatment may not be as effective as Cmpd A in the long-term down-regulation of these genes in this model. Mechanistically, this effect may be attributed to the observation that Cmpd A administration strongly inhibited the inflammatory influx, which would in turn translate to a reduction in the mRNA levels of genes expressed by these cell types. Additionally, as PGD_2-mediated CRTH2 activation occurs early in the allergic inflammatory cascade, blockade of this interaction would be expected to have broad downstream effects, inhibiting both the recruitment of inflammatory cell types as well as mediators produced. This is in contrast to the mechanism of action of the steroid Dex, which inhibits the transcription factor NF-AT. Along these same lines, GPR44/CRTH2 did not appear to be down-regulated by Dex treatment at all in this FITC model compared with Cmpd A.

In summary, an examination of cytokine and chemokine RNA and protein levels suggests that multiple pathways underlie the FITC-induced inflammation and are regulated, in part, the CRTH2 activation. These reductions in cytokines and chemokines are consistent with the gross reduction in ear thickness observed, as well as the histology, which shows a rather limited inflammatory infiltrate upon treatment with the higher doses (1 and 10 mg kg^{-1}) of Cmpd A. Taken together, these observations underscore the pivotal role of the CRTH2–PGD$_2$ interaction in regulating allergen-induced cutaneous inflammation. However, a complete reduction in pro-inflammatory mediators was not observed with Cmpd A administration. This may be due, in part, to other pro-inflammatory mediators released by activated mast cells or the pharmacokinetic/pharmacodynamic profile of Cmpd A in mice. Nonetheless, these observations suggest that an overall reduction, but not necessarily a complete abrogation, of pro-inflammatory cytokine and chemokine production may be sufficient to severely dampen the cutaneous inflammatory response and the ensuing tissue pathology. Further, these studies suggest that antagonism of CRTH2 may be a potentially useful strategy in the therapeutic intervention of allergic disease.

Abbreviations

AD	atopic dermatitis
Cmpd A	Compound A
CRTH2	chemoattractant receptor-homologous molecule expressed on T_h2 cells
Dex	dexamethasone
H and E	hematoxylin and eosin
IHC	immunohistochemistry
mRNA	messenger RNA
PGD$_2$	prostaglandin D$_2$
qPCR	quantitative PCR
RT	reverse transcription
SEM	standard error of the mean
TARC	T cell-attracting chemokine
TGF-β	transforming growth factor-β
TNF-α	tumor necrosis factor-α
TSLP	thymic stromal lymphopoietin
Veh	vehicle

References

1 Bieber, T. 2008. Atopic dermatitis. *N. Engl. J. Med.* 358:1483.
2 Leung, D. Y. 1999. Pathogenesis of atopic dermatitis. *J. Allergy Clin. Immunol.* 104:S99.
3 Ou, L. S. and Huang, J. L. 2007. Cellular aspects of atopic dermatitis. *Clin. Rev. Allergy Immunol.* 33:191.
4 Iwasaki, M., Nagata, K., Takano, S., Takahashi, K., Ishii, N. and Ikezawa, Z. 2002. Association of a new type prostaglandin D2 receptor CRTH2 with circulating T helper 2 cells in patients with atopic dermatitis. *J. Invest. Dermatol.* 119:609.
5 Hamid, Q., Boguniewicz, M. and Leung, D. Y. 1994. Differential *in situ* cytokine gene expression in acute versus chronic atopic dermatitis. *J. Clin. Invest.* 94:870.
6 Liu, Y. J., Soumelis, V., Watanabe, N. *et al.* 2007. TSLP: an epithelial cell cytokine that regulates T cell differentiation by conditioning dendritic cell maturation. *Annu. Rev. Immunol.* 25:193.
7 Allakhverdi, Z., Comeau, M. R., Jessup, H. K. *et al.* 2007. Thymic stromal lymphopoietin is released by human epithelial cells in response to microbes, trauma, or inflammation and potently activates mast cells. *J. Exp. Med.* 204:253.
8 Yoo, J., Omori, M., Gyarmati, D. *et al.* 2005. Spontaneous atopic dermatitis in mice expressing an inducible thymic stromal lymphopoietin transgene specifically in the skin. *J. Exp. Med.* 202:541.
9 Li, M., Messaddeq, N., Teletin, M., Pasquali, J. L., Metzger, D. and Chambon, P. 2005. Retinoid X receptor ablation in adult mouse keratinocytes generates an atopic dermatitis triggered by thymic stromal lymphopoietin. *Proc. Natl Acad. Sci. USA* 102:14795.
10 Chan, L. S., Robinson, N. and Xu, L. 2001. Expression of interleukin-4 in the epidermis of transgenic mice results in a pruritic inflammatory skin disease: an experimental animal model to study atopic dermatitis. *J. Invest. Dermatol.* 117:977.
11 Takeshita, K., Yamasaki, T., Akira, S., Gantner, F. and Bacon, K. B. 2004. Essential role of MHC II-independent CD4+ T cells, IL-4 and STAT6 in contact hypersensitivity induced by fluorescein isothiocyanate in the mouse. *Int. Immunol.* 16:685.
12 Tang, A., Judge, T. A., Nickoloff, B. J. and Turka, L. A. 1996. Suppression of murine allergic contact dermatitis by CTLA4Ig. Tolerance induction of Th2 responses requires additional blockade of CD40-ligand. *J. Immunol.* 157:117.
13 Boyce, J. A. 2007. Mast cells and eicosanoid mediators: a system of reciprocal paracrine and autocrine regulation. *Immunol. Rev.* 217:168.

14 Kim, N. and Luster, A. D. 2007. Regulation of immune cells by eicosanoid receptors. *Scientific WorldJournal* 7:1307.

15 Pettipher, R., Hansel, T. T. and Armer, R. 2007. Antagonism of the prostaglandin D2 receptors DP1 and CRTH2 as an approach to treat allergic diseases. *Nat. Rev. Drug Discov.* 6:313.

16 Sugimoto, H., Shichijo, M., Iino, T. *et al.* 2003. An orally bioavailable small molecule antagonist of CRTH2, ramatroban (BAY u3405), inhibits prostaglandin D2-induced eosinophil migration *in vitro. J. Pharmacol. Exp. Ther.* 305:347.

17 Nagata, K., Tanaka, K., Ogawa, K. *et al.* 1999. Selective expression of a novel surface molecule by human Th2 cells *in vivo. J. Immunol.* 162:1278.

18 Hirai, H., Tanaka, K., Yoshie, O. *et al.* 2001. Prostaglandin D2 selectively induces chemotaxis in T helper type 2 cells, eosinophils, and basophils via seven-transmembrane receptor CRTH2. *J. Exp. Med.* 193:255.

19 Lucaks, N., Berlin, A. A., Franz-Bacon, K. *et al.* 2008. CRTH2 antagonism significantly ameliorates airway hyperreactivity, and down-regulates inflammation-induced genes in a mouse model of airway inflammation. *Am. J. Physiol. Lung Cell. Mol. Physiol.* 295:L767.

20 Sásik, R., Woelk, C. H. and Corbeil, J. 2004. Microarray truths and consequences. *J. Mol. Endocrinol.* 33:1.

21 Cole, S. W., Galic, Z. and Zack, J. A. 2003. Controlling false-negative errors in microarray differential expression analysis: a PRIM approach. *Bioinformatics* 19:1808.

22 Takeshita, K., Yamasaki, T., Nagao, K. *et al.* 2004. CRTH2 is a prominent effector in contact hypersensitivity-induced neutrophil inflammation. *Int. Immunol.* 16:947.

23 Shichijo, M., Sugimoto, H., Nagao, K. *et al.* 2003. Chemoattractant receptor-homologous molecule expressed on Th2 cells activation *in vivo* increases blood leukocyte counts and its blockade abrogates 13,14-dihydro-15-keto-prostaglandin D2-induced eosinophilia in rats. *J. Pharmacol. Exp. Ther.* 307:518.

24 Ott, N. L., Gleich, G. J., Peterson, E. A., Fujisawa, T., Sur, S. and Leiferman, K. M. 1994. Assessment of eosinophil and neutrophil participation in atopic dermatitis: comparison with the IgE-mediated late-phase reaction. *J. Allergy Clin. Immunol.* 94:120.

25 Cookson, W. 2004. The immunogenetics of asthma and eczema: a new focus on the epithelium. *Nat. Rev. Immunol.* 4:978.

26 Li, A. G., Lu, S. L., Han, G., Hoot, K. E. and Wang, X. J. 2006. Role of TGF-β in skin inflammation and carcinogenesis. *Mol. Carcinog.* 45:389.

27 Biedermann, T., Kneilling, M., Mailhammer, R. *et al.* 2000. Mast cells control neutrophil recruitment during T cell-mediated delayed-type hypersensitivity reactions through tumor necrosis factor and macrophage inflammatory protein 2. *J. Exp. Med.* 192:1441.

28 Dilulio, N. A., Engeman, T., Armstrong, D., Tannenbaum, C., Hamilton, T. A. and Fairchild, R. L. 1999. Gro alpha-mediated recruitment of neutrophils is required for elicitation of contact hypersensitivity. *Eur. J. Immunol.* 29:3485.

29 Liu, Y. J. 2006. Thymic stromal lymphopoietin: master switch for allergic inflammation. *J. Exp. Med.* 203:269.

30 Rochman, I., Watanabe, N., Arima, K., Liu, Y. J. and Leonard, W. J. 2007. Cutting edge: direct action of thymic stromal lymphopoietin on activated human CD4+ T cells. *J. Immunol.* 178:6720.

31 Omori, M. and Ziegler, S. F. 2007. Induction of IL-4 expression in CD4+ T cells by thymic stromal lymphopoietin. *J. Immunol.* 178:1396.

32 Imai, Y., Kondo, A., Iizuka, H., Maruyama, T. and Kurohane, K. 2006. Effects of phthalate esters on the sensitization phase of contact hypersensitivity induced by fluorescein isothiocyanate. *Clin. Exp. Allergy* 36:1462.

33 Ebner, S., Nguyen, V. A., Forstner, M. *et al.* 2007. Thymic stromal lymphopoietin converts human epidermal Langerhans cells into antigen-presenting cells that induce proallergic T cells. *J. Allergy Clin. Immunol.* 119:982.

34 Bogiatzi, S. I., Fernandez, I., Bichet, J. C. *et al.* 2007. Cutting edge: proinflammatory and Th2 cytokines synergize to induce thymic stromal lymphopoietin production by human skin keratinocytes. *J. Immunol.* 178:3373.